

# Mechanical Properties Of Calcium Carbonate Crystallization Of Chitin Reinforced Polymer

Michael Ikpi Ofem, Muneer Umar, Musa Muhammed

**ABSTRACT:** Chitin whiskers and  $\text{CaCO}_3$  were reinforced with Poly(acrylic acid). Mechanical and thermal properties were characterised. The effect of  $\text{CaCO}_3$  growth on the mechanical properties of chitin whiskers reinforced Poly(acrylic acid) indicated that better mechanical properties can be achieved at chitin content of 3 wt % when compared with neat PAA. The growth of  $\text{CaCO}_3$  on CHW/PAA composite increased the melting endotherm of CHW/PAA/ $\text{CaCO}_3$  composite when compared with CHW/PAA composite. As an indication of increase in thermal stability, the final weight loss at the end of decomposition for all composites was between 20 and 37 %, far below the 78 % for the CHW/PAA composite and 84 % for the pure PAA .

**Keywords:** calcium carbonate, chitin whiskers, filler loading, Mechanical properties, polymorphs.

## 1.0 INTRODUCTION

Research into the biomimetic synthesis of  $\text{CaCO}_3$  in the presence of additives has been on the increase. One major reason for the research is to get a clue on how the production of organised organic or inorganic materials with complex morphologies can be achieved by biomineralization. A new hybrid of organic or inorganic materials with distinct properties and structures can be obtained if the correct polymer material is used. Morphological control of  $\text{CaCO}_3$  crystallisation using organic templates can also lead to the formation of different shapes Hosoda and Kato, (2001); Park and Meldrum, (2002); Küther *et al.*, (1998); Walsh and Mann, (1995); Qi *et al.*, (2002). The polymorphism of  $\text{CaCO}_3$  crystallised in the presence of chitin or its derivative chitosan as substrates and PAA as a soluble additive was found to form different morphologies Kato and Amamiya, (1999); Sugawara and Kato, (2000); Hosoda and Kato, (2001); Wada *et al.*, (2004); Kotachi *et al.*, (2006). In the same vein, the crystallization of  $\text{CaCO}_3$  in the presence of PAA without a substrate like chitin or chitosan also produced different polymorphs. The differences have been attributed to molecular weights [Huang *et al.*, (2008)], concentration of PAA [Dalas and Koutsoukos, (1989); He *et al.*, (2009)] and the temperature of crystallization [Ouhenia *et al.*, (2008)]. Different nanoscale fillers have shown to enhance the mechanical and thermal properties of nanocomposites [Fu and Qutubuddin, (2001); Zhane *et al.*, (2003); Ma *et al.*, (2007)]. These properties include Young modulus, strength, impact performance and heat resistance. The mechanical properties of chitin or chitosan reinforced calcium carbonate polymer composites have been reported [Abdolmohammadi *et al.* (2012); Eirasa and Pessan, (2009); Ihueze *et al.*, (2011)]. These reports show that the tensile modulus increases with  $\text{CaCO}_3$  nanoparticle loading. A gradual improvement with the addition of up to 1 wt% of nano-sized  $\text{CaCO}_3$  on the tensile strength and elongation at break was previously reported by Abdolmohammadi *et al.* (2012). Similarly, Eirasa and Pessan (2009) reported an increase in

elastic modulus and a little increase in yield stress for Polypropylene/Calcium Carbonate nanocomposites compared with the matrix Polypropylene, though a reduction in brittle-to-ductile transition temperature and an increase in impact resistance with the addition of nanoparticles. Here,  $\text{CaCO}_3$  crystallisation in the presence of CHW at different filler loading with PAA as a soluble additive is reported.

## 2.0 Experimental methodology

### 2.1 Preparation of Chitin whiskers CHW/PAA/ $\text{CaCO}_3$ composites.

Preparation of  $\text{CaCO}_3$  and CHW/PAA/ $\text{CaCO}_3$  composites was prepared as reported elsewhere Ofem, (2015) while 0.3wt % chitin whiskers (CHW) were prepared as reported by Junkasem, *et.al.*, (2010); Junkasem, Rujiravanit, and Supaphol, (2006); Morin, and Dufresne, (2002). Prepared 0.2M of  $\text{K}_2\text{CO}_3$  and 0.2M of  $\text{CaCl}_2$  at a ratio of 1:1 by volume were mixed in a beaker at 30 °C for 5 minutes while stirring. The solid precipitate, obtained immediately after mixing the two solutions, was collected by filtrations. The collected precipitate was rinsed three times with deionised water. The  $\text{CaCO}_3$  precipitates were dried in an oven at 100 °C for 1 hour, resulting in finely grained powder. To incorporate  $\text{CaCO}_3$  into the composite, 5ml of  $\text{K}_2\text{CO}_3$  and 5ml of  $\text{CaCl}_2$  were mixed with various weight fractions of CHW and PAA. The CHW/PAA/ $\text{CaCO}_3$  in the beaker was heated at 30°C for 5 minutes. The CHW/PAA/ $\text{CaCO}_3$  solution was poured in a plastic petri dish and allowed to dry in a fume hood and later in the oven. The final volume before drying was maintained at 60 ml. The weight fractions of CHW used were 0.73, 0.42, 0.23, 0.11 and 0.03.

## 3.0 Result and Discussions

### 3.1 Mechanical Properties

One major reason for poor mechanical properties in nanocomposites is poor dispersion of nanofillers with

agglomerates constituting the weak points. The degree of dispersion in the matrix will greatly affect the mechanical and thermal properties of the composites and ease the transfer of the intrinsic properties of the. Another reason for poor mechanical and thermal properties is the interfacial interaction between the nanoparticles and the polymer matrix. Figure 1 shows stress- strain curves of chitin film while figure 2 is that of PAA and figure 3 for CHW/PAA/CaCO<sub>3</sub> composites. From the stress-strain curve PAA shows plastic behaviour. The stress whitening and necking behaviour of PAA could be seen at low filler loading of CHW (3%cw and 11%cw), this behaviour disappears at higher filler loading. The addition of CaCO<sub>3</sub> imparts a brittle behaviour on the composite.

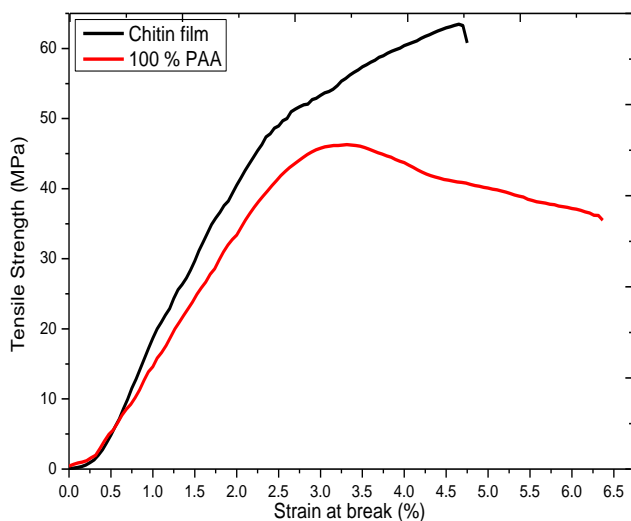


**Figure 1 - Typical stress-strain curves of chitin and Poly(acrylic acid) films**

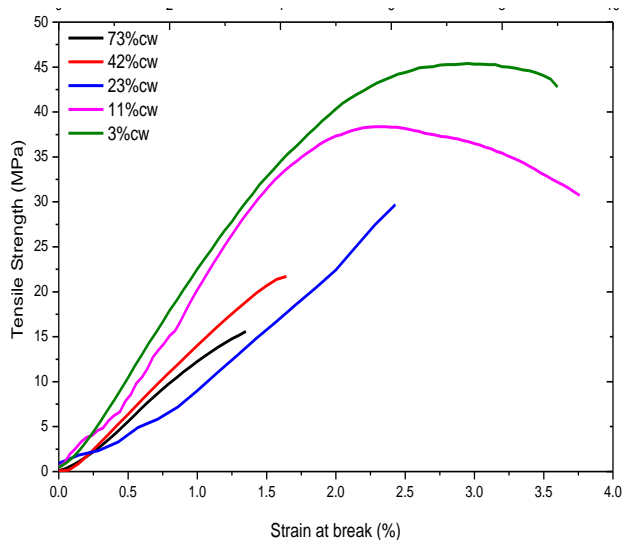


**Figure 2 - Typical stress-strain curves of CHW/25PAA/CaCO<sub>3</sub> composites at different loading levels of whiskers.**

The strain at break reduces by 50 % when compared with the neat PAA in the presence of CaCO<sub>3</sub> and by 47.5 % in the absence of CaCO<sub>3</sub>. The decrease is an indication of increase in brittleness in the presence of CaCO<sub>3</sub>. The tensile strength at 3%cw increases from 35.3 MPa for neat PAA to 36.4 MPa for CHW/PAA Ofem, (2015) and to 42.8 MPa for CHW/PAA/CaCO<sub>3</sub> composite. An increase of 17.7 and 20.1% respectively. The improved tensile strength induced by Ca<sup>2+</sup> ions at this filler level arise from ionic interactions between the multiple binding sites introduced by CHW/PAA and divalent Ca<sup>2+</sup> ions. It has been reported by Walther *et al.*, (2010); Hartmann *et al.*, (2009) that randomly distributed ionic bonds can play a role in enhancing bond formation in bio-based composites. In the same vein, the increase in modulus in the presence of CaCO<sub>3</sub> at this level of CHW content must be caused by the interaction between the polymer matrix and the fillers due to the large interfacial area between the particles [Chan *et al.*, (2002); Chen *et al.*, (2004)]. The presence of nano-sized CaCO<sub>3</sub> with high surface area improves the cross-linking between the polymer, CHW and the Ca<sup>2+</sup>. This cross-linking increased the modulus. From table 1 it can be seen that at higher CHW content there was no improved mechanical properties. At higher filler loading dispersion of CaCO<sub>3</sub> will be difficult; this is because nanoparticles with high surface area tend to agglomerate [Yang *et al.*, (2006)], resulting to debonding from the matrix. Once a particle debonds, it will be difficult, if not impossible, for stress transfer to take place as none of the debonded particles can carry any fraction of the external load. The inability of the debonded particles to carry any load will lead to poor properties.

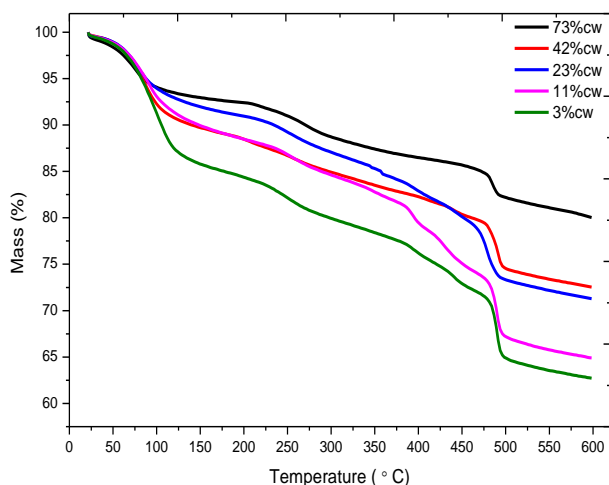
**Table 1 - Mechanical properties of CHW/PAA/CaCO<sub>3</sub>**

Sample	Tensile Strength (MPa)	Strain at break (%)	Modulus (GPa)
Chitin	60.8(1.3)	4.5(0.4)	2.7(0.4)
100%PAA	35.3(2.5)	6.4(0.4)	2.0(0.3)
3%cw	36.4(2.2)	5.9(0.8)	1.9(0.2)
11%cw	43.6(3.2)	4.6(1.2)	2.8(0.2)
23%cw	34.7(2.8)	4.5(0.5)	2.5(0.8)
42%cw	21.5(2.4)	2.9(0.2)	2.9(0.2)
73%cw	17.8(2.5)	2.6(0.3)	2.7(0.3)

### 3.2 Thermogravimetric Analysis (TGA/DTG)

Figures 3 and 4 show the TGA and DTG curves of the CHW/25PAA/CaCO<sub>3</sub> composites, respectively. From the TGA curves two major weight loss stages are observed for all the composites. The 1<sup>st</sup> stage occurs between 50-200 °C with a maximum decomposition rate occurring at 74°C and a weight loss of between 4 and 5 % as the wt. % of CHW decreases. Such weight losses are assigned to loss of

physically absorbed moisture. The addition of  $\text{CaCO}_3$  reduces the weight loss to 5 % as against ~7 % when  $\text{CaCO}_3$  was absent. Ofem, (2015). The weight loss at the end of this stage is between 5 and 12 %. The second major weight loss is between 425 and 550 °C with maximum rates at 487, 490, 491, 491 and 491°C as CHW content decreases. This weight loss is due to degradation of saccharide rings and the depolymerisation and decomposition of both acetylated and deacetylated units of chitin in addition to full degradation of the chains of PAA. The % weight losses at the end of the stage are respectively ~19, 27, 28, 34 and 36. The addition of  $\text{CaCO}_3$  increases the thermal stability as the amount of chitin whiskers decreases.



**Figures 3** - TGA curves of CHW/PAA/ $\text{CaCO}_3$  composites

The decomposition rate increased from between 419 and 434 °C Ofem, (2015) in the absence of  $\text{CaCO}_3$  to 487 °C for 73%cw and between 443 and 491 °C, for 42%cw, 23%cw, 11%cw and 3%cw, an increase of between 6 and 16 %. From the DTG thermograms (figure 4) broad peaks are observed at 274 and 256 °C for 73%cw and 42%cw respectively. Another broad peak was observed at 443 °C for 23%cw, 11%cw and 3%cw. The decomposition of chitin Ofem, (2015) showed two decomposition stages; the 1<sup>st</sup> between 51-120 °C with a maximum decomposition rate at 83 °C and a weight loss of 4 wt %. The next degradation occurred between 257-391 °C at a maximum decomposition rate of 362 °C, corresponding to a weight loss of 28 %. This stage was described as the degradation of saccharide rings and the depolymerisation and decomposition of the acetylated and deacetylated units of chitin [Peniche *et al.*, (1993); Kim *et al.*, (1994)]. The final weight loss at the end of the degradation of chitin was 51 wt %. For 100% PAA a three-stage degradation process occurred. These decomposition stages occurred at 50-162, 217-294 and 362-464 °C with the decomposition rates at 143, 273 and 392 °C corresponding to weight losses of 7, 26 and 80% respectively. From the CHW/PAA composites

Ofem, (2015) the maximum decomposition rate increases from 83 to 127 °C for the 1<sup>st</sup> stage of decomposition with a weight loss of between 4 and 7 %. The decomposition rate for the second stage was 272° C with the weight losses ranging between 45 and 67 %. The decomposition rate for the third stage occurs between 419 and 434 °C with a final weight loss reducing to 78 % at 73%cw. When  $\text{CaCO}_3$  was incorporated there was a drastic change in weight losses. For the 1<sup>st</sup> stage of weight loss, a sharp peak occurred at 74 °C which typically is attributed to loss of water. Contrary to the CHW/PAA composites, there was no sharp peak from the DTGA curves for CHW/PAA/ $\text{CaCO}_3$  composites, rather a very small broad peaks were observed, but this time, at lower temperatures (251-256°C) compared to the peak at 443°C. These broad peaks could be attributed to the decomposition of chitin and PAA [Yamamoto *et al.*, (2010)]. Baitalov *et al.*(1998) and Popescu *et al.*(2014) reported that the exothermic peak at ~ 459°C correlates with a vaterite-calcite phase transition. In this research work, vaterite/calcite transitional peaks probably correspond with those observed at 487, 490, 491, 491 and 491°C as CHW weight decreases. The final weight loss at the end of the decomposition was between 20 and 37 %, far below the 78 % for the CHW/PAA composite and 84 % for the pure PAA.  $\text{CaCO}_3$  decomposes to  $\text{CaO}$  between 500 and 790 °C with weight loss of between 43 and 44 %. [Tanaka and Naka, (2010); Popescu *et al.*, (2014)]. The final weight loss of between 20 and 37 % in this research work indicates that the decomposition of  $\text{CaCO}_3$  within this temperature range (0-600 °C) did not take place. These could have contributed to the increase in thermal stability due to increase in cross-linking between the polymers and  $\text{CaCO}_3$ . Figure 5 shows the weight loss of the materials.

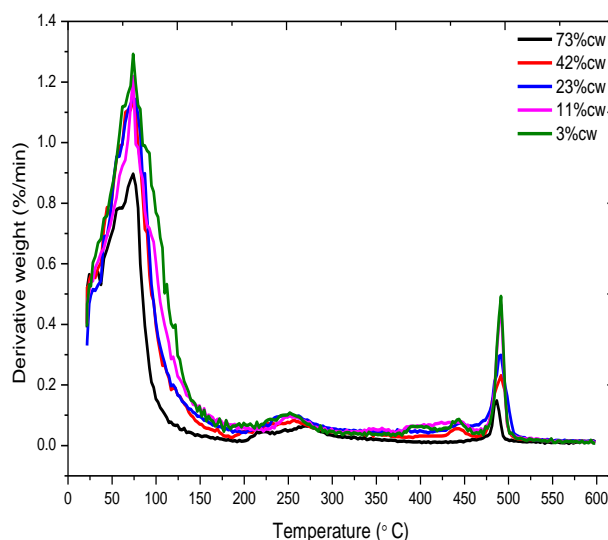


**Figure 4**- DTGA curves of CHW/PAA/ $\text{CaCO}_3$  composites

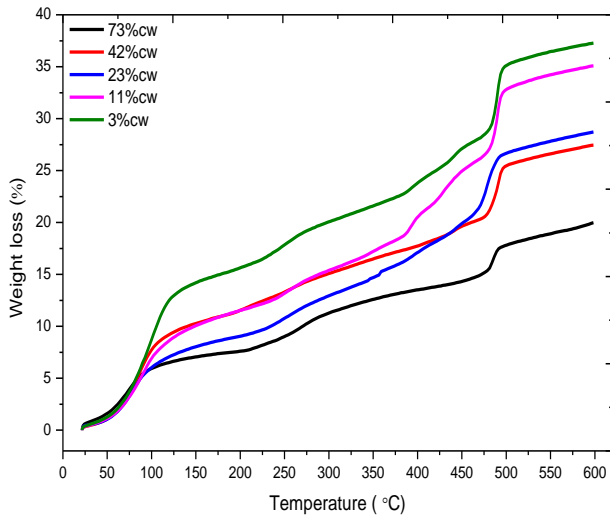


Figure 5 - Weight loss of CHW/PAA/CaCO<sub>3</sub> composites

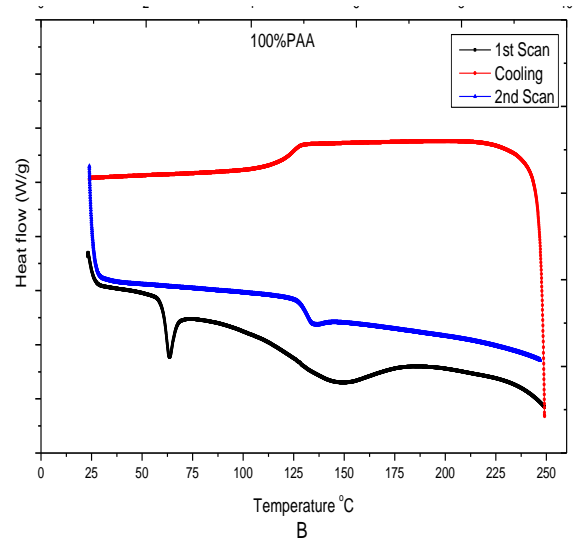
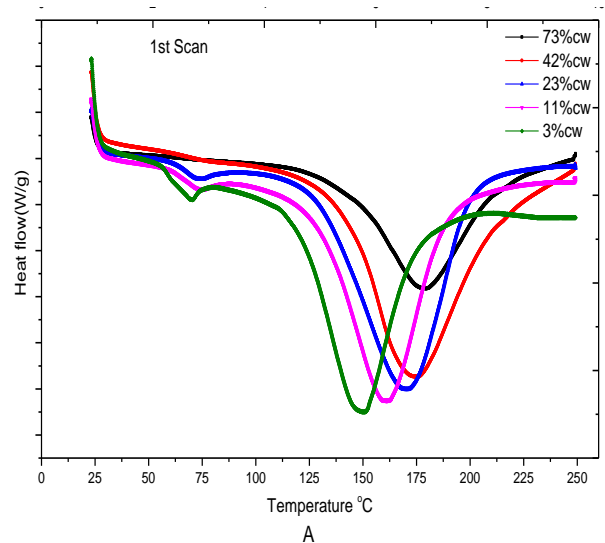
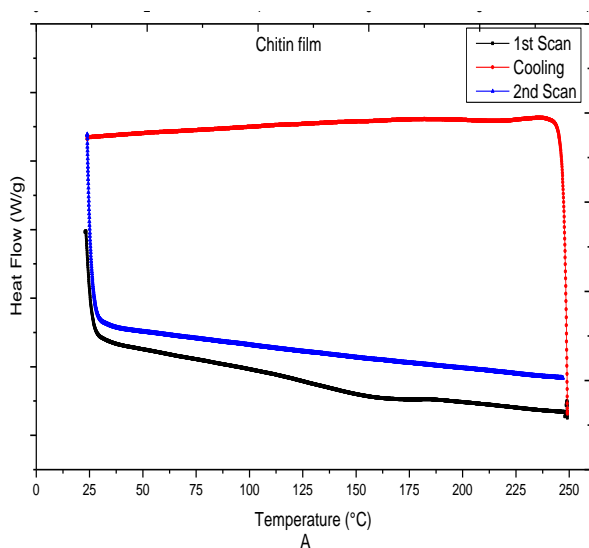


Figure 6 - DSC heating curves of (A) chitin film and (B) poly(acrylic acid)

3.3 DSC Analysis

Figures 6 show the DSC profiles of chitin and PAA. Chitin did not show any glass transition confirming earlier reports by Kurita *et al.*, (2002); Kim *et al.*, (1994). A weak endothermic peak attributed to the evaporation of bounded water [Jang *et al.*, (2004)] was observed. The discrepancies of the  $T_g$  of PAA depends on the medium of solvent, the molecular weight and the drying time and temperature prior to characterisation [Park *et al.*, (1991); Maurer *et al.*, (1987); Al-Najjar M *et al.*, (1996)]. The first heat of PAA gave a  $T_g$  of ~58 °C with a melting endothermic temperature of ~ 146 °C. For the second heating cycle, the glass transition at 135 °C was observed. The change in  $T_g$  from 58 °C to 135°C is a confirmation of dehydration of bound water which has a plasticizing effect.

Figure 7 shows the DSC profile of CHW/PAA/CaCO<sub>3</sub> composites (A) 1<sup>st</sup> heating scan, (B) cooling scan and (C) the 2<sup>nd</sup> heating scan. Tables 2 and 3 show the glass transition temperature ( $T_g$ ) and melting endotherm ( $T_m$ ) of CHW/PAA/CaCO<sub>3</sub> composites and the crystallization temperature ( $T_c$ ) of chitin, PAA and CHW/PAA composites, respectively. The second scan of all composites did not show any  $T_g$ ,  $T_m$  or  $T_c$ . From the two tables no  $T_g$  was observed for higher CHW content (73%cw and 42%cw). However, there was a slight increase in  $T_g$  compared with the neat PAA. The shape of the  $T_g$  inflections become more broad as the CHW content increases and disappears at higher filler loading.



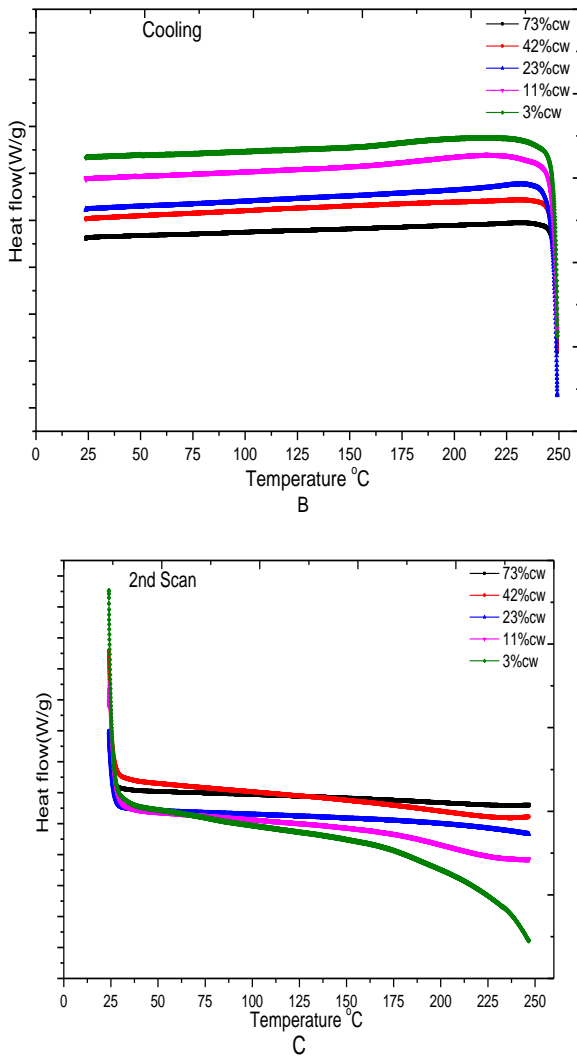


**Figure 7 - DSC heating curves of CHW/PAA/CaCO<sub>3</sub> composites (A) 1<sup>st</sup> scan (B) cooling and (C) 2<sup>nd</sup> scan**

The increase in  $T_g$  indicates that there is some level of interaction. The increase from 58°C for neat PAA to 64°C in the presence of CaCO<sub>3</sub> could also mean reduction of polymer chain flexibility and interaction energy between molecules [Gumfekar *et al.*, (2011); Tigli and Evren, (2005)]. From the cooling curves (figure 7) it can be seen that crystallisation did not take place when CaCO<sub>3</sub> was incorporated. In the absence of CaCO<sub>3</sub>, CHW/PAA crystallisation peaks were observed at ~129 °C of fem, (2015). This shows that the incorporation of CaCO<sub>3</sub> interferes with crystal growth

**Table 2 -  $T_g$  and  $T_m$  of and CHW/PAA /CaCO<sub>3</sub> composites**

Sample ID	$T_g$ (°C)	$T_m$ (°C)
73%cw	-	176.5(4.2)
42%cw	-	175.4(3.3)

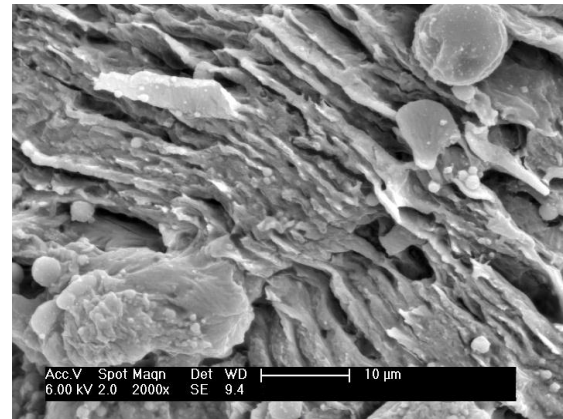
23%cw	64.4(3.2)	165.2(3.5)
11%cw	64.3(3.3)	160.5(2.5)
3%cw	61.6(2.2)	148.5(3.3)

**Table 3 -  $T_g$ ,  $T_m$ , and  $T_c$  of 25PAA, chitin and CHW/PAA Composites [ Ofem, (2015)]**

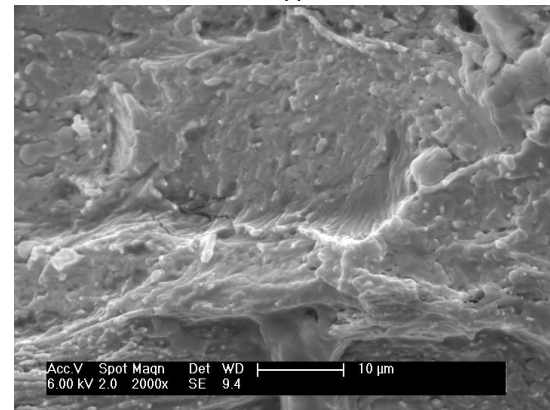
Sample	1st Scan		2nd Scan Cooling	
	$T_g$ (°C)	$T_m$ (°C)	$T_g$ (°C)	$T_c$ (°C)
Chitin	-	-	-	-
100%PA A	58.2(1.7)	146.1(3,2)	134.8(0.5)	129.3(0.7)
73%cw	54.1(1.4)	126.4(4.7)	-	-
42%cw	60.5(0.3)	127.3(0.9)	142.4(2.1)	140.9(2.5)
23%cw	59.7(1.3)	136.9(0.7)	136.3(0.3)	128.2(0.1)
11%cw	57.1(0.4)	141.2(0.5)	135.1(0.2)	129.2(0.5)
3%cw	57.3(0.7)	143.6(0.8)	135.2(0.4)	129.6(0.1)

The absence of crystallisation can be discussed based on the report of Lin *et al.*, (2004). When CaCO<sub>3</sub> was incorporated into polypropylene (PP) and then modified by acrylic acid (AA), it was observed that at lower content of AA, the nucleation effect of CaCO<sub>3</sub> was weakened, leading to a lower crystallisation temperature. The argument given was based on the dosage of AA used. The surface area of CaCO<sub>3</sub> used was 23.24m<sup>2</sup>/g. If AA tends to orient normal to the filler surface area with the carboxylic groups, one molecule of AA will occupy 0.2 nm<sup>2</sup> area. Since the surface area of CaCO<sub>3</sub> was 23. 24 m<sup>2</sup>/g, AA will need 11.62 x10<sup>19</sup> molecules/g or 0.18 mmol/g to form a monolayer coating equivalent to 1.38 phf (parts per hundred of filler). This dosage was below the used quantity (2, 4 and 6phf) in the research, indicating an over dosage of AA. When a lower content of AA (2phf) was used, the peak melting temperature slightly reduced, however at higher content (6phf) the peak melting temperature increases. The authors postulated that at lower AA content, since the crystallization temperature was low, crystals with small lamellar thickness were formed; at higher AA content the lamellar thickness increased due to increase in crystallization temperature which eventually increases the peak of melting temperature. The addition of dicumyl peroxide (DCP), irrespective of AA content, lowered the peak melting temperature but the decrease was not significant. Tabtiang and Venables(1999) investigated the effect of AA content on the crystallization of PP at various contents of DCP and the stabilizer trimethylolpropane trimethacrylate (TMP). The

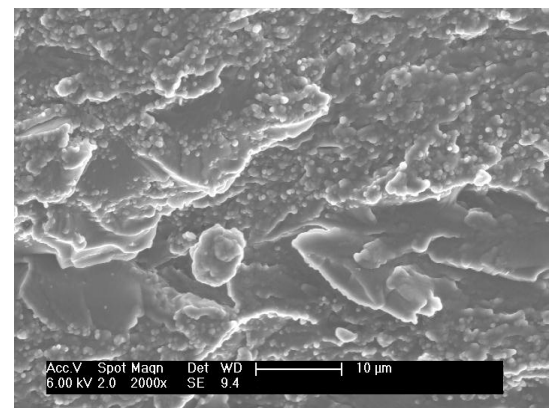
results showed that the crystallization temperature increased as the AA content increased while increase in DCP and TMP, decreases the crystallization temperature. In this research work, the quantity of  $\text{CaCO}_3$  was kept constant while CHW and PAA were varied. At lower PAA the nucleation effect of  $\text{CaCO}_3$  will be low, at higher PAA;  $\text{CaCO}_3$  will react with PAA to form  $\text{PAA-Ca}^+$ . This reaction will lead to improved heterogeneous nucleation and an increase in the crystallization temperature of PAA in the CHW/PAA/ $\text{CaCO}_3$  composites. From figure 7, a careful observation reveals a downward slope curve of 23%cw to 3%cw. This slope is conspicuous for 3%cw where the highest PAA content was used. The non-appearance of crystallization here could be attributed to the low dosage of PAA. Following the reports of Lin *et al.*, (2004) and Tabtiang and Venables, (1999), it is expected that the melting temperature at higher PAA content to be higher than at lower PAA content, however the reverse was seen. The reason for this behaviour is not certain and therefore, subject to further investigations. However a relaxation temperature of 236 °C for  $\alpha$ -chitin has been reported by Kim *et al.*, (1994) while Jang *et al.*,(2004) using DSC to characterise  $\alpha$ ,  $\beta$  and  $\gamma$  chitin reported decomposition temperatures of 330, 230 and 310 °C, respectively. Prashanth *et al.*(2002), reported a peak temperature and enthalpy of fusion ( $\Delta H$ ) of shrimp chitin at 139 °C and 158 J/g respectively. Other authors who reported a change in slope of chitin curves are Kittur *et al.*, (2002), at ~125 °C, Peesan *et al.*, (2003), at 120 °C for  $\beta$  chitin and Yen and Mau, (2007) at 248 °C. When  $\text{CaCO}_3$  was not grown on the composite, the melting endotherms were lower at lower contents of PAA as can be seen from table 3. The incorporation of  $\text{CaCO}_3$  may have brought about the relaxation temperature of chitin there by increasing the melting temperature of CHW/PAA/ $\text{CaCO}_3$  composites at lower CHW. **Figure 8** shows SEM micrographs of the fracture surfaces of CHW/PAA/ $\text{CaCO}_3$  composites. 3%cw fracture surface shows relatively smooth cross section devoid of lamellar layers. Both rhombohedral calcite and needle-like aragonite can be seen. A lamellar surface fracture was observed for 73%cw with traces of spherical vaterite. White spots of  $\text{CaCO}_3$  particles with traces of cavities indicate weak bonding between the filler and the matrix. These cavities translate to voids in 73%cw resulting in the poor mechanical properties as reported here. Plastic deformation failure is evident in all samples.



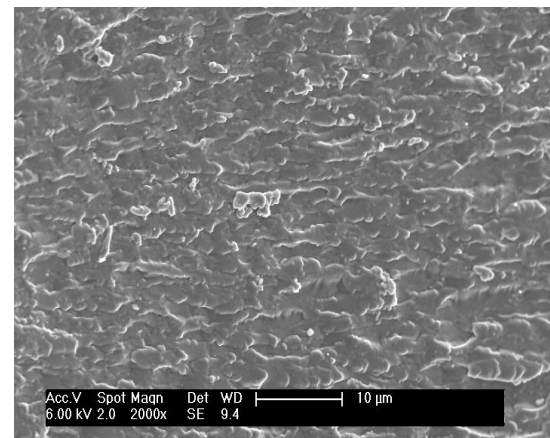
A



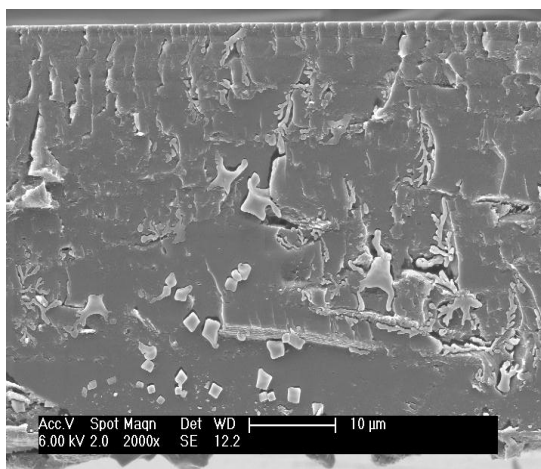
B



C



D



E

**Figure 8** - SEM images of fracture surfaces of Figure 8 - SEM images of fracture surfaces of (A) 72%cw (B) 42%cw (C) 23%cw (D) 11%cw and (E) 3%cw.

### 3.4 Conclusions

The effects of  $\text{CaCO}_3$  growth on the mechanical and thermal properties of CHW reinforced PAA at different loading of CHW and PAA were examined. Better mechanical properties were measured for CHW loading of 3%cw compared with neat PAA and when  $\text{CaCO}_3$  was not incorporated (CHW/PAA). The failure mode was more plastic at lower filler loading of CHW. TGA indicated that the composites thermal stabilities were increased. At each stage of decomposition the weight losses were lower than those without  $\text{CaCO}_3$ . The final weight losses were between 20 and 37 % compared with over 70 % when  $\text{CaCO}_3$  was not grown on the composites, a char yield of over 60 % was obtained. The  $T_g$  values increase from that of 58 °C for neat PAA to between 61 and 64°C compared with a maximum of 60°C when  $\text{CaCO}_3$  was absent. The crystallization temperatures for all composites were not observed and this was attributed to the low quantity of PAA used.

### References

- [1] Hosoda, N and Kato, T,( 2001). Thin-Film Formation of Calcium Carbonate Crystals: Effects of Functional Groups of Matrix Polymers. *Chemistry of Materials*13: 688-693.
- [2] Park, R.J and Meldrum, F.C, (2002). Synthesis of Single Crystals of Calcite with Complex Morphologies. *Advanced Materials*14:1167-1169.
- [3] Küther, J. Seshadri, R. Tremel, W, (1998). Crystallization of Calcite Spherules around Designer Nuclei. *Angewandte Chemie International Edition* 37: 3044-3047.

- [4] Walsh, D and Mann, S,(1995). Fabrication of hollow porous shells of calcium carbonate from self-organizing media. *Nature* 377:320-323.
- [5] Qi, J. Li, J and Ma J, (2002). Biomimetic morphogenesis of calcium carbonate in mixed solutions of surfactants and double-hydrophilic block copolymer. *Advanced Materials* 14:300-303.
- [6] Kato T and Amamiya T, (1999). A new approach to organic/inorganic composites. Thin film coating of  $\text{CaCO}_3$  on chitin fibre in the presence of acid-rich macromolecules. *Chemistry letters* 199-200.
- [7] Sugawara A and Kato T, (2000). Aragonite  $\text{CaCO}_3$  thin-film formation by cooperation of  $\text{Mg}^{2+}$  and organic polymer matrices. *Chemical Communications* 487-488.
- [8] Wada N, Suda S, Kanamura K and Umegaki T,(2004). Formation of thin calcium carbonate films with aragonite and vaterite forms coexisting with poly(acrylic acids) and chitosan membranes. *Journal of Colloidal Interface Science* 277:167-174.
- [9] Kotachi A, Miura T, and Imai H,(2006). Polymorph Control of Calcium Carbonate Films in a Poly(acrylic acid)-Chitosan System. *Crystal Growth and Design* 6:1636-1641.
- [10] Huang S, Naka K and Chuj Y, (2008). Effect of molecular weights of poly(acrylic acid) on crystallization of calcium carbonate by delayed addition method. *Polymer Journal* 40:154-162.
- [11] Dalas E and Koutsoukos PG, (1989). The crystallization of vaterite on cholesterol. *Journal of Colloidal Interface Science* 127:273-280.
- [12] He L, Xue R and Song R, (2009). Formation of calcium carbonate films on chitosan substrates in the presence of poly(acrylic acid). *Journal of Solid State Chemistry* 182:1082-1087.
- [13] Ouheniaa S, Chateigner D, Belkhiria M, Guilmeaub E and Kraussb C, (2008). Synthesis of calcium carbonate polymorphs in the presence of polyacrylic acid. *Crystal growth* 310:2832-2841.
- [14] Fu X, Qutubuddin S, (2001). Polymer-clay nanocomposites: Exfoliation of organophilic montmorillonite nanolayers in polystyrene. *Polymer* 42:807-813.

- [15] Zhang W, Chen D, Zhao Q and Fang Y, (2003). Different vinyl acetate content on the morphology and properties of eva/clay nanocomposites. *Polymer* 44:7953-7961.
- [16] Ma CG, Mai YL, Rong MZ, Ruan WH and Zhang MQ, (2007). Phase structure and mechanical properties of ternary polypropylene/elastomer/nano-CaCO<sub>3</sub> composites. *Composite Science Technology* 67:2997-3005.
- [17] Abdolmohammadi S, Samira S, Ibrahim NA, Yunus W, Rahman M, Azizi S and Fatehi A, (2012). Enhancement of Mechanical and Thermal Properties of Polycaprolactone/Chitosan Blend by Calcium Carbonate Nanoparticles. *International Journal of Molecular Science* 13:4508-4522.
- [18] Eirasa D and Pessan LA, (2009). Mechanical Properties of Polypropylene/Calcium Carbonate Nanocomposites. *Materials Research* 12(4): 517-522.
- [19] Ihueze C C, Mgbemena CO and Sylvester, Ugwu, (2011). The Influence of Creep on the Mechanical Properties of Calcium Carbonate Nanofiller Reinforced Polypropylene. *Journal of Minerals & Materials Characterization & Engineering* 10(2):143-159.
- [20] Ofem, M (2015). Properties of chitin whisker reinforced poly(acrylic acid) composites, PhD Thesis, School of Materials, The University of Manchester.
- [21] Junkasem J, Rujiravanit R and Supaphol P, (2006). Fabrication of  $\alpha$ -Chitin Whisker Reinforced Poly(vinylalcohol) Nanocomposite Nanofibers by Electrospinning. *Nanotechnology* 17:4519-4528.
- [22] Junkasem J, Rujiravanit R, Grady BP and Supaphol P, (2010). X-Ray Diffraction and Dynamic Mechanical Analyses of  $\alpha$ -Chitin Whisker-Reinforced Poly (vinyl alcohol) Nanocomposite Nanofibers. *Polymer International* 59:85-91.
- [23] Morin A and Dufresne A, (2002). Nanocomposites of Chitin Whiskers from Riftia Tubes and Poly(caprolactone). *Macromolecules* 35:2190-2199.
- [24] Walther A, Bjurhager I, Malho JM, Ruokolainen J and Berglund L and Ikkala O, (2010). Supramolecular Control of Stiffness and Strength in Lightweight High-Performance Nacre-Mimetic Paper with Fire-Shielding Properties. *Angewandte Chemie International Edition* 49:6448-6453.
- [25] Hartmann MA and Fratzl P, (2009). Sacrificial Ionic Bonds Need To Be Randomly Distributed To Provide Shear Deformability. *Nano Letters* 9:3603-3607.
- [26] Chan CM, Wu J, Li JX and Cheung YK, (2002). Polypropylene/calcium carbonate nanocomposites. *Polymer* 43:2981-2992.
- [27] Chen N, Wan C, Zhang Y and Zhang Y, (2004). Effect of nano-CaCO<sub>3</sub> on mechanical properties of PVC and PVC Blendex blend. *Polymer Testing* 23:169-174.
- [28] Yang K, Yang Q, Li G, Sun Y and Feng D, (2006). Morphology and mechanical properties of polypropylene/calcium carbonate nanocomposite. *Materials Letters* 60:805-809.
- [29] Peniche C, Argüelles-Monal W, Davidenko N, Sastre R, Gallardo A and San Román J, (1999). Self-curing membranes of Chitosan/PAA IPNs obtained by Radical Polymerization: Preparation, Characterization and Interpolymer Complexation. *Biomaterials* 20:1869-1875.
- [30] Kim S, Kim S, Moon Y and Lee Y, (1994). Thermal characteristics of chitin and hydroxypropyl chitin. *Polymer* 35:3212-3216.
- [31] Yamamoto Y, Nishimura T, Saito T and Kato T, (2010). CaCO<sub>3</sub>/chitin-whisker hybrids: formation of CaCO<sub>3</sub> crystals in chitin-based liquid-crystalline suspension. *Polymer Journal* 42:583-596.
- [32] Baitalow F, Wolf G and Schmidt HG, (1998). Thermochemical investigation of calcium carbonate phase transitions I. Thermal activated vaterite-calcite transition. *Journal of Thermal Analysis* 52:5-16.
- [33] Popescu M, Isopescu R, Matei C, Fagarasan G and Plesu V, (2014). Thermal decomposition of calcium carbonate polymorphs precipitated in the presence of ammonia and alkylamines. *Advanced Powder Technology* 25:500-507.
- [34] Tanaka Y and Naka K, (2010). A carbonate controlled-addition method for size-controlled calcium carbonate spheres by carboxylic acid-terminated poly(amidoamine) dendrimers *Polymer Journal* 42: 676-683.



- [35] Kurita K, Inoue M and Harata M, (2002). Graft Copolymerization of Methyl Methacrylate onto Mercaptochitin and Some Properties of the Resulting Hybrid Materials. *Biomacromolecules* 3:147-152.
- [36] Jang M, Kong B, Jeong Y, Lee CH and Nah J, (2004). Physicochemical Characterization of  $\alpha$ -Chitin,  $\beta$ -Chitin, and  $\gamma$ -Chitin Separated from Natural Resources. *Journal of Polymer Science: Part A: Polymer Chemistry* 42:3423-3432.
- [37] Park J, Kim D and Kim C, (1991). Effect of Drying condition on the glass transition of Poly(acrylic acid). *Polymer Engineering and Science* 36:867-872.
- [38] Maurer J, Eustace D and Ratcliffe CT, (1987). Thermal characterization of poly(acrylic acid). *Macromolecules* 20:196-202.
- [39] Al-Najjar M, Hamid S and Hamad E, (1996). The glass transition temperature of nitrated polystyrene/poly(acrylic acid). *Polymer Engineering and science* 36:2083-2087.
- [40] Gumfekar SP, Kunte KJ, Ramjee L, Kate KH, Sonawane SH, (2011). Synthesis of  $\text{CaCO}_3$ -P(MMA-BA) nanocomposite and its application in water based alkyd emulsion coating. *Progress in Organic Coatings* 72:632- 637.
- [41] Tigli RS and Evren V, (2005). Synthesis and characterization of pure poly(acrylate) latexes. *Progress in Organic Coatings* 52:144-150.
- [42] Lin Z, Huang Z, Zhang Y, Mai K and Zeng H, (2004). Crystallization and Melting Behaviour of Nano- $\text{CaCO}_3$ /Polypropylene Composites Modified by Acrylic Acid. *Journal of Applied Polymer Science* 91:2443-2453.
- [43] Tabtiang A and Venables R, (1999). Effect of coagent in reactive surface treatment for calcium carbonate filler in polypropylene. *Plastic, Rubber and Composites* 28:11-19.
- [44] Prashanth K, Kittur F and Tharanathan R, (2002). Solid state structure of chitosan prepared under different N-deacetylating conditions. *Carbohydrate Polymers* 50:27-33.
- [45] Kittur F, Prashanth K, Sankar K and Tharanathan R, (2002). Characterization of chitin, chitosan and their carboxymethyl derivatives by differential scanning calorimetry. *Carbohydrate Polymer* 49:185-193.
- [46] Peesan M, Rujiravanit R and Supaphol P, (2003). Characterisation of  $\beta$ -chitin/poly(vinyl alcohol) blend film. *Polymer Testing* 22:381-387.
- [47] Yen M and Mau J, (2007). Selected physical properties of chitin prepared from shiitake stripes. *LWT* 40:558-563.